



Laser assisted bioprinting of engineered tissue with high cell density and microscale organization

Bertrand Guillotin ^{a,*}, Agnès Souquet ^a, Sylvain Catros ^a, Martí Duocastella ^b, Benjamin Pippenger ^a, Séverine Bellance ^a, Reine Bareille ^a, Murielle Rémy ^a, Laurence Bordenave ^a, Joëlle Amédée ^a, Fabien Guillemot ^a

^a INSERM U577 Biomaterials and Tissue Repair, Université Victor Segalen Bordeaux 2, 146 rue Léo Saignat, zone Nord, Bâtiment 4a, 2^{ème} étage, 33076 Bordeaux cedex, France
^b Universitat de Barcelona, Departament de Física Aplicada i Òptica Martí i Franqués 1, 08028-Barcelona, Spain

ARTICLE INFO

Article history:

Received 21 April 2010

Accepted 21 May 2010

Available online 2 July 2010

Keywords:

Tissue engineering
Laser assisted bioprinting
Laser manufacturing
Rapid prototyping
Micropatterning
High cell density printing

ABSTRACT

Over this decade, cell printing strategy has emerged as one of the promising approaches to organize cells in two and three dimensional engineered tissues. High resolution and high speed organization of cells are some of the key requirements for the successful fabrication of cell-containing two or three dimensional constructs. So far, none of the available cell printing technologies has shown an ability to concomitantly print cells at a cell-level resolution and at a kHz range speed. We have studied the effect of the viscosity of the bioink, laser energy, and laser printing speed on the resolution of cell printing. Accordingly, we demonstrate that a laser assisted cell printer can deposit cells with a microscale resolution, at a speed of 5 kHz and with computer assisted geometric control. We have successfully implemented such a cell printing precision to print miniaturized tissue like layouts with *de novo* high cell density and micro scale organization.

© 2010 Elsevier Ltd. All rights reserved.

1. Introduction

Biological tissues are composed of multiple components in close interactions with each other: different cell types, each embedded in their specific extracellular matrix and with blood capillaries nearby. Cells are often in physical contact with each other, which allows complex interactions which support homeostasis. The development of strategies to reproduce the functional anisotropy of living tissue remains a puzzling challenge for tissue engineers. The winning strategy may address precise organization of different cell types embedded in cell type specific ECM with specific growth factors, cell adhesion proteins and specific mechanical properties.

Parallel to the scaffold based strategy involving cell seeding onto porous structures, the bioprinting approach aims at building three dimensional biological structures or functional organs, layer-by-layer, from the bottom up [1,2]. Jet-based methods to print living cells have been reviewed previously [3,4]. Among them, the Laser

Induced Forward Transfer (LIFT) technique allows printing inorganic as well as organic material with micrometer resolution. Initially developed to transfer metals [5], the LIFT has been successfully modified to print biological material such as peptides, DNA, and cells [6–8]. A LIFT based bioprinter designed to print biological material was created and named BioLP (Biological Laser Printer) by Barron et al. [9]. LIFT based bioprinters or Laser Assisted Bioprinters (LAB) are comprised of three components [3]: (i) a pulsed laser source, (ii) a target, or ribbon, from which a biological material is printed, and (iii) a receiving substrate that collects the printed material. In brief, the ribbon is made of a thin absorbing layer of metal (such as gold or titanium) coated onto a laser transparent support (*i.e.* glass). Organic material (molecules or cells) is prepared in a liquid solution (*i.e.* culture media), and deposited at the surface of the metal film. The laser pulse induces vaporization of the metal film, resulting in the production of a jet of liquid solution which is deposited onto the facing substrate [1,10].

The highest resolution of cell printing could be defined as a continuous line-up of cells, in which successive cells are printed one by one at desired coordinates, and in contact with each other. Such a micro scale cell printing resolution implies that the cell fraction of each printed droplet should tend to 100%.

Considering the LAB, the resolution of printing, *i.e.* the size and proximity of the printed droplets, depends on parameters like the

* Corresponding author. Tel.: +33 557579273; fax: +33 556900517.

E-mail addresses: bertrand.guillotin@insERM.fr (B. Guillotin), agnes.souquet@insERM.fr (A. Souquet), sylvain.catros@hotmail.com (S. Catros), marti_duocastella@ub.edu (M. Duocastella), bennippenger@hotmail.com (B. Pippenger), severine.bellance@gmail.com (S. Bellance), reine.bareille@insERM.fr (R. Bareille), murielle.remy@u-bordeaux2.fr (M. Rémy), laurence.bordenave@biophys.u-bordeaux2.fr (L. Bordenave), joelle.amedee@insERM.fr (J. Amédée), fabien.guillemot@insERM.fr (F. Guillemot).

thickness of the layer of the bioink coated onto the ribbon, the surface tension and the viscosity of the bioink, the wettability of the substrate, the laser fluence, the air gap between the ribbon and the substrate [1]. The compromise between these parameters in order to obtain the desired resolution of printing may thus vary depending on the type of material being printed. The influence of these parameters on jet formation is still under investigation [11,12]. Therefore, controlled cell printing (*i.e.* absence of splashing, controlled size of the liquid droplet) by LAB remains challenging and the highest resolution of cell printing has not yet been attained.

According to the bioprinting approach, the resolution counterbalances the volume criterion [13]. For a given volume to fabricate, given a constant printing speed, increasing the organization of the said volume would be more time consuming. Particular attention should then be brought to the printing speed, when high throughput production of a micro scale resolution material is desired. For this reason, our experiments were all performed using a laser pulse repetition rate $f = 5$ kHz.

Our objective was i) to study the effect of viscosity, cell density, laser energy and laser printing speed to attain the highest resolution of cell printing at $f = 5$ kHz, ii) to use this high resolution of cell printing to print a tissue-like interface in one sequence of multiple cell type printing, and iii) to implement high resolution of cell printing into tissue fabrication by laser printing.

2. Material and method

2.1. Laser-assisted bioprinter

The laser-assisted bioprinting workstation has been described previously [13]. Briefly, the laser source is a solid Nd:YAG crystal laser (Navigator I, Newport Spectra Physics, 1064 nm wavelength, 30ns pulse duration, 1–100 kHz repetition rate, 7 W mean power). A large field optical F-theta lens (58 mm focal length, S4LFT, Sill Optics, France) is used to focus the laser beam onto the titanium film surface. The laser beam is driven by a scanning system composed of two galvanometric mirrors (SCANgine 14, ScanLab), with a scanning speed reaching 2000 mm/s. A 5-axis carousel system has been integrated into the workstation (NovaLase, S.A., Canéjan, France) with the purpose of printing multi-color patterns. Substrate positioning, carousel driving, video observation and pattern designs are monitored with dedicated software. The transfer process was performed in air, at room temperature, with a distance of 400 μm between the ribbon and the substrate. Glass slides were used as substrate. Depending on the experiment, cells were printed directly onto the glass slide, or on a 100 μm thick layer of a solution of 90 mg/ml fibrinogen (see below). All experiments were performed using a repetition rate of 5 kHz. The laser energy deposit can be modulated by tuning the laser power (6–80 mW) or the diaphragm aperture stop (5–18 mm).

2.2. Cell line

Rabbit carcinoma cell line B16, and Human umbilical vein endothelial cell line Eahy926 were cultured on plastic dishes in Iscove modified Dulbecco's medium (IMDM, GIBCO, Life Technologies, France) supplemented with 10% fetal bovine serum (Boehringer, Mannheim, Germany), in a controlled atmosphere (5% CO_2 , 100% humidity, 37 °C).

2.3. Bioink preparation

Cells were suspended in Dulbecco's Modified Eagle Medium (DMEM). Depending on the experiment, this cell suspension was supplemented with varying concentration of glycerol (v/v) and varying concentration of sodium alginate (w/v; Protanal 10/60 – FMC BioPolymer), or with Matrigel™ (see below), or with a solution of thrombin (see below).

2.4. Viscosity measurement

The viscosity of different bioinks was measured with a controlled stress rheometer (AR1000, TA instruments).

2.5. Ribbon preparation

A 50 nm thick titanium film was deposited under vacuum on a glass slide with a Peltier cooled sputter coater (K575X, Emitech). Three micro litters of bioink per cm^2 were spread onto the metal film using a blade coater (3570 Elcometer).

2.6. Tissue fabrication into Matrigel™

Matrigel was purchased from BD Biosciences. It was diluted in DMEM to a final concentration of 4 mg/ml to resuspend cells or to be served as 100 μm thick substrate onto the glass slide.

2.7. Tissue fabrication into fibrin hydrogel

Tissucol Kit (Baxter) has been prepared according to manufacturer's instructions. A solution of thrombin (250 UI) and CaCl_2 (40 mM) was used 1:1 to resuspend cells in order to make a bioink with a cell concentration of $5 \cdot 10^7$ to 10^8 cells/ml. A fibrinogen solution was prepared at a concentration of 90 mg/ml and served as a 100 μm thick substrate onto the glass slide.

2.8. Cell viability

Cell viability was assessed 24 h post printing using live/dead assay (Invitrogen) according to manufacturer's instructions.

2.9. Image analysis

Ribbon and substrate were observed after each printing experiment with a Nikon Optiphot-2 inverted optical microscope equipped with a Sony PowerHAD 3CCD color video camera driven by Matrox Intellacam software, or with a Nikon Eclipse 80i equipped with a motorized stage. Blind 3-D deconvolution with 15 iterations was performed on the z-stack pictures with Autoquant 2.2.0 software. Three-dimensional reconstruction with surface mode was performed with Imaris 7.0.0 software.

3. Results

3.1. Viscosity and laser energy deposit influence the printing resolution

The viscosity of different bioinks is shown in Table 1. Forty million cells/ml adds 20% of the viscosity to a 1% (w/v) alginate solution. Results in Table 2 show that the ejected droplet diameter onto the substrate is correlated to the viscosity of the bioink and the laser energy deposit. The higher the viscosity and/or the lesser the energy deposit, the smaller the droplet diameter will be. It is possible to achieve similar resolution, *i.e.* similar droplet size, with a 0.1% (w/v) alginate bioink printed with a laser pulse energy of 6 μJ (droplet size: $49 \pm 3.5 \mu\text{m}$), and with a 1% alginate (w/v) bioink printed with a pulse energy of 12 μJ (droplet size: $51 \pm 4.2 \mu\text{m}$). These results show that the printing resolution depends on the bioink viscosity and the laser energy deposit.

3.2. High cell concentration for high cell printing resolution

The effect of the cell suspension viscosity on printing resolution was addressed. Cell suspensions supplemented with or without 1% (w/v) alginate were compared (Fig. 1). Cells were printed at a concentration of 50 million cells/ml, according to the pattern of the Olympic flag. Results show some splashing in the absence of alginate (Fig. 1a). In the presence of 1% (w/v) alginate, splashing is reduced (Fig. 1b). One percent alginate increased the solution viscosity up to 100 mPa s. With such a viscosity, splashing of the bioink onto the substrate is reduced, and the resolution of the printed pattern is increased.

Table 1

Viscosity of culture media supplemented with alginate, glycerol, and cells. Glycerol is added into the bioink to prevent evaporation. The cell model used in this experiment is the rabbit carcinoma cell line B16, at a concentration of $4 \cdot 10^7$ cells/ml. Experiment was carried on at 10 °C.

Solution in culture media (DMEM)	Viscosity (mPa s)
Alginate 0.5% w/v; glycerol 30% v/v	50
Alginate 1% w/v	100
Alginate 1% w/v; glycerol 30% v/v	110
Alginate 1% w/v; $4 \cdot 10^7$ cells/ml	120

Table 2

Diameter of the ejected droplet onto the glass substrate, depending on alginate concentration in the bioink, and laser energy (μJ). The different bioinks were composed of mQ water supplemented with 30% (v/v) glycerol, with varying concentration of alginate. c: coalescence of contiguous droplets onto the substrate. n.t.: no transfer of the bioink onto the substrate.

Alginate	4.5 μJ	6.0 μJ	7.5 μJ	9.0 μJ
0.1% w/v	49 \pm 3 μm	69 \pm 3 μm	c	c
0.5% w/v	38 \pm 3 μm	55 \pm 5 μm	64 \pm 5 μm	62 \pm 6 μm
1.0% w/v	n.t.	48 \pm 4 μm	46 \pm 3 μm	51 \pm 4 μm

Different laser parameters were tested on two cell concentrations: 50 million cells/ml and 100 million cells/ml (Fig. 2). Using 18 or 11 mm diaphragm (D) and 16 μJ energy (E), the printed droplets coalesced onto the substrate and formed a continuous line of bioink. Decreasing laser energy deposit by using a $D = 5$ mm and $E = 16 \mu\text{J}$, the printed droplets were smaller and remained individualized. The higher the energy deposited, the wider the printed cell line would become. As a result, bigger droplets were printed in which cells were more likely to be dragged off by draining/capillary effect (Fig. 2, upper left panel, $D = 18\text{--}11$ mm). At $5 \cdot 10^7$ cells/ml with $D = 5$ mm and $E = 16 \mu\text{J}$, some droplets were printed without a cell (Fig. 2, upper left panel, diaphragm aperture stop $D = 5$ mm). With cell concentration of 10^8 cells/ml, at least one cell was present in each printed droplet (Fig. 2, upper right panel, $D = 5$ mm), thus increasing cell printing resolution. No printed droplet was observed using $D = 5$ mm in combination with $E = 8 \mu\text{J}$.

3.3. Cell printing resolution according to the laser scanning speed

We have studied the effect of the laser scanning speed on the cell printing resolution. Cells were prepared at a concentration of

10^8 cells/ml in culture medium. At 1600 and 800 mm/s, consecutive droplets were individualized and distant from 300 and 160 μm respectively, as anticipated (Fig. 3a). At 400 and 200 mm/s, the distance between printed droplets was seemingly shorter. We did not see any resolution improvement between 200 and 100 mm/s (Fig. 3a,b). The results at 1600 and 800 mm/s show that each printed droplet contained at least one cell (Fig. 3b). In these experimental conditions, we found the best resolution of cell printing was achieved using a scanning speed of 200 mm/s.

3.4. High spatial resolution allows precise multi cell type spatial arrangement

Fig. 4 illustrates the multi-color printing capability of the LAB. Two distinct suspensions of cells (human endothelial cell lineage Eahy 926, 60 million cells/ml) were sequentially printed in 2 dimensions according to a pattern of two concentric circles (Fig. 4a). The inner circle was printed first using a suspension of cells loaded with green fluorescent calcein (Fig. 4b). Secondly, the outer circle was printed using a suspension of cells loaded with red fluorescent Dil-LDL (Fig. 4c). Differential staining of the cells revealed the two circles overlapped, which was likely due to bioink coalescence between the two circles. This experiment shows that different cell types can be printed in close contact to each other, with a high cell concentration, according to a desired spatial organization.

3.5. LAB application to living tissue fabrication

We used the LAB to print a stable soft free form structure with a resolution compatible with microvasculature dimensions (Fig. 5). A solution of fibrinogen (90 mg/ml) was served as biopaper onto the glass substrate. The ribbon was loaded with a bioink made of a solution of thrombin and CaCl₂ (250 UI and 40 mM respectively). The bioink was then printed onto the fibrinogen according to a network of parallel and perpendicular lines (dimension: 2 \times 2 cm, pitch: 500 μm). With laser scanning speed set at 200 mm/s, this 4 cm^2 pattern was printed in a couple of seconds.

This result was reproduced using the same bioink supplemented with Eahy926 endothelial cell line ($6 \cdot 10^7$ cells/ml). The cell containing bioink was printed according to a matrix of parallel lines (Fig. 6a). A live/dead assay staining was performed 24 h after the printing experiment (Fig. 6c). Virtually all the printed cells concentrated calcein and excluded ethidium homodimer, and were thus considered viable. The distribution of the printed cells embedded in the fibrin pattern was measured within a depth of 100 μm into the fibrinogen layer (Fig. 6d). Similar experiment has been reproduced using 4 mg/ml Matrigel into the bioink and as a 100 μm thick substrate (not shown).

4. Discussion

We have demonstrated that cells can be printed at a microscale resolution and at a high speed: a 10^8 cells/ml concentrated bioink, with a viscosity of at least 120 mPa s can be processed by the LAB to print cells almost one by one, next to each other. Because the printing speed is also critical for living tissue fabrication [13], we have performed all of our experiments using a laser pulse repetition rate of 5 kHz. In our experiments, the laser energy deposit needed to be tightly adjusted with respect to the viscosity and the cell concentration of the bioink. Accordingly, a wide range of extracellular matrices, characterized by as many different viscosities (within the range studied) can be printed at a similar resolution. This is in agreement with previously described mechanism of bioink droplet ejection (see [1] for a review). Thanks to this

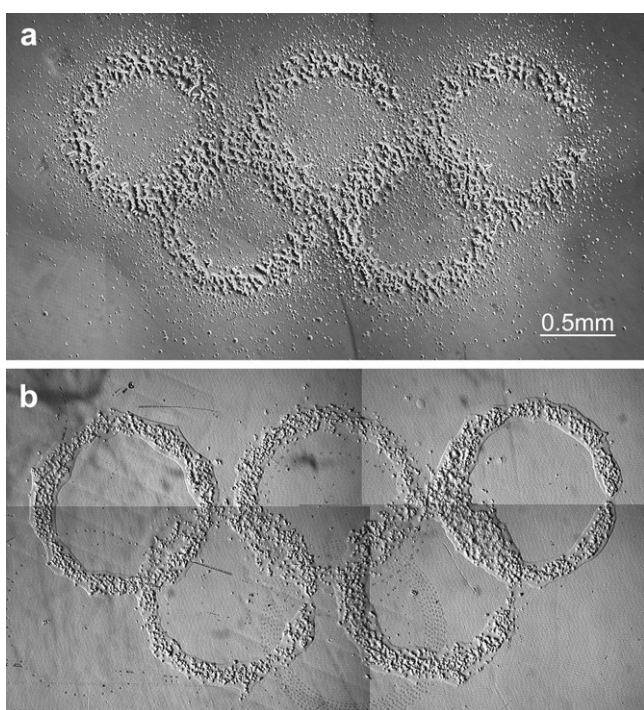


Fig. 1. Cellularized 2D pattern resolution according to viscosity. Fifty million cells per ml were suspended in DMEM supplemented with 10% glycerol (a), plus 1% (w/v) alginate (b). Satellite droplets (splashing) are virtually absent when 1% (w/v) alginate is added to the bioink. Phase contrast microscope image of cells printed onto glass. Magnification 25 \times .

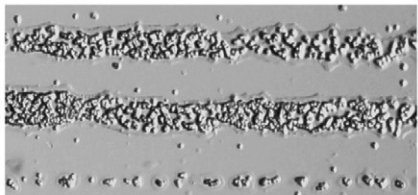
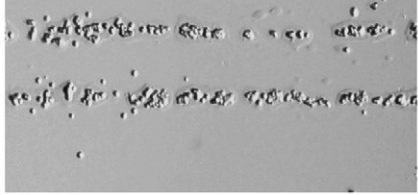
$5 \cdot 10^7$ cells/ml	$1 \cdot 10^8$ cells/ml	mm	μJ
		_18	
		_11	16
		_5	
		_18	
		_11	8
		_5	

Fig. 2. Cell printing resolution according to the cell concentration of the bioink (DMEM, 1% aginate (w/v), 5% glycerol), the diaphragm aperture stop (mm) and the laser energy deposit (μJ). Phase contrast microscope image of cells printed onto glass. Magnification 25 \times .

microscale resolution, we have fabricated high cell density tissue like constructs with micro scale organization.

The high printing resolution of liquids achieved by LAB has been demonstrated [7,10,14]. It is well established that cells can be printed using the LAB. To achieve microscale cell printing precision, cells should be printed with a minimal volume of surrounding ECM (or bioink). However, cell printing is statistic [15,16]. The presence of a single cell in each printed droplet is challenged by the use of a bioink with a low cell concentration (e.g. $5 \cdot 10^7$ cells/ml in our

hands). We hypothesized that the LAB should be able to print cells one by one, next to each other. We have adjusted the cell concentration onto the ribbon, the laser parameters according to the viscosity of the bioink, so that cells were printed within a droplet volume as small as possible. Inkjet printers and plotters are able to print cells and sub millimeter sized objects (e.g. cell aggregates [17]). Regarding cell printing, some limitations have been described like printer head clogging issues due to cell concentration of the bioink superior to 10^7 cells/ml. We have demonstrated that the LAB can print a high cell fraction per droplet volume (*i.e.* cells with little surrounding bioink volume). Accordingly, the LAB can print cells one by one from a high cell concentration bioink (10^8 cells/ml), to fabricate a tissue engineered product with comparable organization and cell density with living tissues in which cells are in physical contact with each other. Further development may focus on the implementation of a cell recognition scanning technology onto the ribbon prior to printing, so that the laser beam could exactly aim one single cell per pulse.

The LAB requires cells to be in a liquid suspension prior to being printed onto the substrate. Moreover, ECM is crucial for cell homeostasis *in vivo*. The cell containing bioink should be composed of an ECM fraction accordingly. Consistent with the layer-by-layer 3D building strategy, the solidification of the bioink onto the substrate is necessary and should be controlled for at least three reasons i) to stabilize the printed 2D pattern, ii) to mechanically support the subsequent bioink layer, iii) to mimic cell type specific extracellular matrix (ECM) with the ability to regulate cell fate [18]. The solidification process of the bioink should not be harmful to the cells. We have supplemented the cell containing bioink with 1% (w/v) alginate hydrogel as a preliminary approach to mimic extracellular matrix. Cell adhesion proteins have been printed successfully since Klebe pioneering work [19,20]. Fibrin is a versatile biopolymer, which presents potential for tissue engineering applications [21]. Cui et al. have recently printed a cellularized pattern reminiscent of microvasculature using an inkjet bioprinter to print cells in combination with fibrin hydrogel [22]. Within the conditions used, a proliferation time of 3 weeks was needed to obtain an endothelium like cell density according to the printed pattern. Printing specificities of inkjetting have been studied previously. To our knowledge, the fastest technology used for a cell printing experiment was 1 kHz using a piezo electric (single printer head) inkjet bioprinter [15], and the highest cell concentration used was 5 million cells/ml [23]. By combining on demand solidification of the printed hydrogel with the high cell printing resolution of the

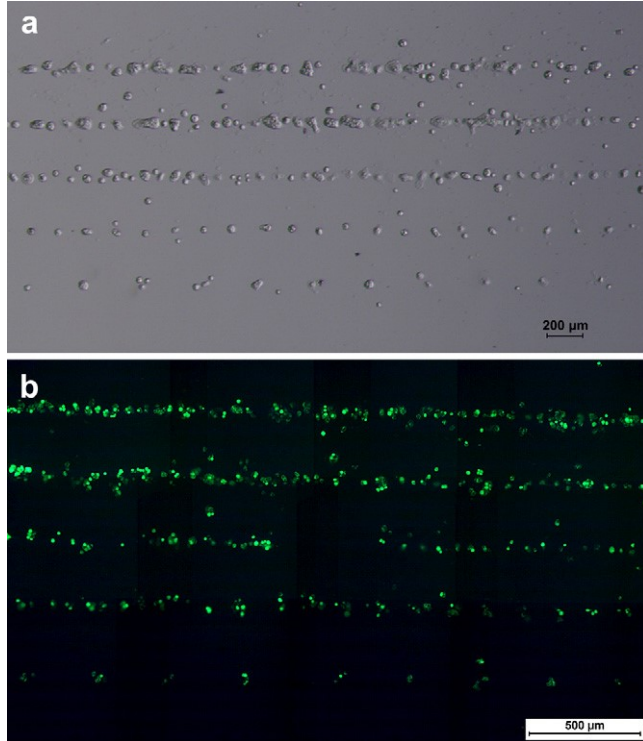


Fig. 3. Cell printing resolution according to the laser scanning speed. Hundred million cells per ml loaded with green fluorescent Calcein-AM (4 μM) were prepared in DMEM. Cells were printed according to five parallel lines of varying scanning speed (from top to bottom): 100; 200; 400; 800 and 1600 mm/s (with laser parameters set at $E = 6 \mu\text{J}$, $D = 11$ mm). (a) Phase contrast microscope image of cells printed onto glass. Scale bar: 200 μm . (b) Fluorescence microscope image of cells printed onto a 100 μm thick layer of Matrigel. Scale bar: 500 μm .

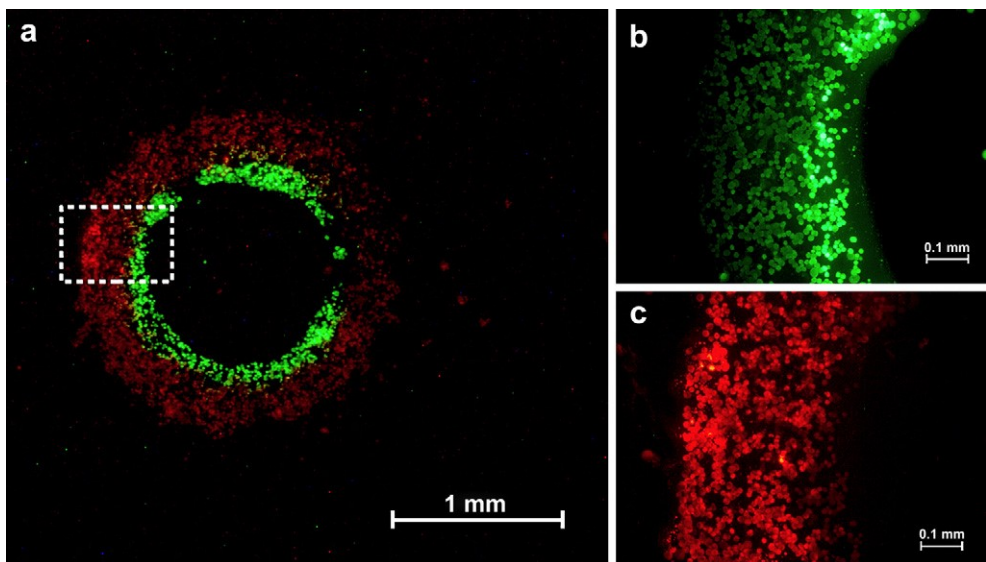


Fig. 4. Sequential two color cell printing in 2D. Human endothelial cell line (Eahy926) was loaded with 4 μ M of green fluorescent Calcein-AM, or with 2 μ g/ml of red fluorescent Dil-LDL prior to the experiment. (a) The two cell suspensions ($6 \cdot 10^7$ cells/ml in DMEM, supplemented with 1% (w/v) alginate were then printed according to a pattern of concentric circles). The two cell suspensions were each blade coated onto two separate ribbons. Both ribbons were placed onto the wheel distributor of the LAB. Calcein loaded cell suspension was used to print the inner circle (1.2 mm diameter). Dil-LDL loaded cell suspension was used to print the outer circle (1.6 mm diameter). (b) Green Calcein stained cells within the region of interest as defined in 4a (dashed rectangle). (c) Red fluorescent Dil-LDL stained cells within the same region of interest. The overlay of Fig. 4b and c shows the two circles partially overlap due to the coalescence of their interface.

LAB as demonstrated herein, we were able to engineer a tissue-like structure with *de novo* high cell density and cell level (microscale) organization. This approach aims at stabilizing cells within a CAD/CAM pattern, and is complementary to bioprinting approach on some homogenous biopaper (i.e. Matrigel) on which random cell migration is allowed [24]. Also, *de novo* high density is required for tissue engineering when using differentiated cells with limited to no potential for proliferation.

Manufacturing of biological structures offers new resources for tissue engineering [25]. Needs for cellular microarrays and high throughput screening techniques have been reviewed [26]. Cell microchips are already available [27], or operational for data production [28,29]. Also, cell sorting technologies with single cell resolution has been reported [30]. Geometrically controlled deposit of cells can be achieved with very high precision based on

dielectrophoretic forces, but extracellular matrix (ECM) deposit can not be controlled by this technology [28]. General needs that a cell microarrayer should fulfill are: fast micro array production, exact controllability of spot position and volume, cost effective production process, and flexibility of printing regarding array layout, microscaling capability (i.e. printing resolution) and versatility of bioink properties (viscosity, cell concentration). These concerns are addressed by the LAB which can process cell concentration (at least 10^8 cells/ml) and viscosity (above 100 mPa s) higher than currently available inkjet bioprinters [3,31]. Such capability allows printing more cells in smaller volumes, with higher level of organization [16,32]. We have shown in this study that the LAB complies with at least two requirements which make it a cell manipulator at micron length scale: 1) it overcomes the traditional trade-off between throughput and positional control, and 2) it is an easy-to-use

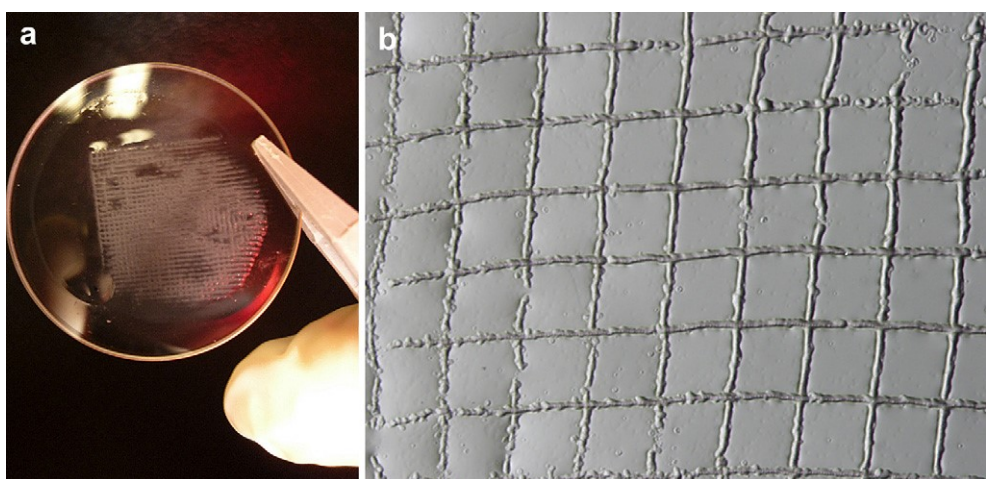


Fig. 5. Geometrically controlled soft free form bioprinting. The bioink composed of thrombin (250 UI) and CaCl₂ (40 mM) has been printed onto a layer of fibrinogen (90 mg/ml), according to a computer designed matrix of parallel and perpendicular lines (2 cm length, 500 μ m pitch). (a) Photograph of the fibrin pattern, scale 1:1. (b) Fibrin pattern observed with a phase contrast optical microscope, magnification 25 \times .

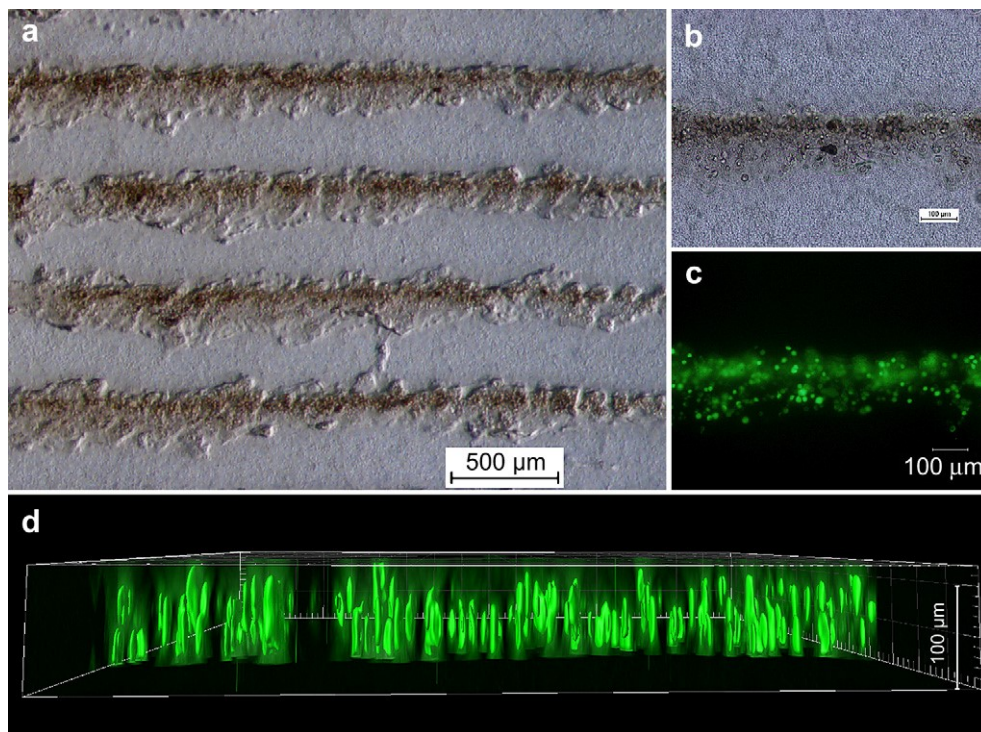


Fig. 6. Geometrically controlled cellularized soft free form bioprinting. Endothelial cell line Eahy926 has been added to the bioink (as detailed in Fig. 5) at a concentration of 6×10^7 cells/ml. The cell containing bioink was then printed on a layer of fibrinogen (90 mg/ml), according to computer designed parallel lines (2 cm in length, 500 μm pitch). (a) Phase contrast optical microscope image, scale bar: 500 μm . (b) Phase contrast optical microscope image, scale bar: 100 μm . (c) Live/dead assay staining of Fig. 6b, fluorescence microscope, scale bar: 100 μm . (d) Orthogonal view of the surface representation of the z-stack of Fig. 6c.

printer that does not require material or cell functionalization [33]. Also, LAB could be integrated into a versatile laser based CAD/CAM system, associating photolithography [34], photo polymerization [35,36], machining, sintering and foaming [37]. All these abilities are suitable for meeting the demand for miniaturization and layout precision for cellular microarray or tissue engineering [31].

Previous studies have shown that LAB allows to print undamaged mammalian cells in terms of viability, DNA damage and function [32,38–41]. The compatibility of our LAB prototype with cell viability has been shown previously [13]. We are currently investigating the functional integrity of the printed cells. Koch et al. have shown that potential deleterious effect of a similar LAB device on printed cells is below detection, if not absent [42].

5. Conclusion

The LAB can print versatile biological patterns such as cell clusters, cell confluent surface and cell alignments according to computer-aided design. Also, a cell-level resolution of cell printing at a high speed (5 kHz) is achievable by this laser assisted bio-printer. Such precision and speed were a prerequisite to apply the LAB to cellularized tissue fabrication. We have shown that printable extracellular matrix and cells can be combined in a laser assisted printing sequence to fabricate a stable and organized soft free form tissue, which can host a high cell density *de novo*. While currently under investigation, control of three-dimensional cell printing strategies should bring LAB to operational maturity in the field of soft free form tissue engineering.

Acknowledgments

The authors gratefully thank Eric Laurichesse (Centre de Recherche Paul Pascal, University of Bordeaux 1) for assistance with rheology

experiments and Stéphanie Lesage for useful talks, to Nicolas Egon (Novalase) for technical support with the laser workstation, to Sébastien Marais for image analysis and to Jean-Christophe Fricain for critical review of the manuscript. M. Duocastella acknowledges funding by MCI of the Spanish Government (Projects MAT2007-62357 and CSD2008-00023), and Fondo Europeo de Desarrollo Regional (FEDER). This study was supported by fundings from GIS “Advanced Materials in Aquitaine” and Région Aquitaine.

Appendix

Figures with essential colour discrimination. Figs. 3–6 in this article have parts that are difficult to interpret in black and white. The full colour images can be found in the online version, at doi:10.1016/j.biomaterials.2010.05.055.

References

- [1] Guillemot F, Souquet A, Catros S, Guillotin B. Laser-assisted cell printing: principle, physical parameters vs. cell fate, and perspectives in tissue engineering. *Nanomedicine* 2010;5:507–15.
- [2] Mironov V, Boland T, Trusk T, Forgacs G, Markwald RR. Organ printing: computer-aided jet-based 3D tissue engineering. *Trends Biotechnol* 2003;21:157–61.
- [3] Ringenstein BR, Othon CM, Barron JA, Young D, Spargo BJ. Jet-based methods to print living cells. *Biotechnol J* 2006;1:930–48.
- [4] Guillemot F, Mironov V, Nakamura M. Bioprinting is coming of ages. *Biofabrication* 2010;2: 2010. 010201.
- [5] Bohandy J, Kim BF, Adrian FJ. Metal deposition from a supported metal film using an excimer laser. *J Appl Phys* 1986;60:1538–9.
- [6] Chrisey DB. Materials processing: the power of direct writing. *Science* 2000;289:879–81.
- [7] Colina M, Serra P, Fernández-Pradas J, Sevilla L, Morenza J. DNA deposition through laser induced forward transfer. *Biosens Bioelectron* 2005;20:1638–42.
- [8] Dinca V, Kasotakis E, Catherine J, Mourka A, Ranella A, Ovsianikov A, et al. Directed three-dimensional patterning of self-assembled peptide fibrils. *Nano Lett* 2008;8:538–43.

- [9] Barron JA, Wu P, Ladouceur HD, Ringeisen BR. Biological laser printing: a novel technique for creating heterogeneous 3-dimensional cell patterns. *Biomed Microdevices* 2004;6:139–47.
- [10] Serra P, Duocastella M, Fernandez-Pradas JM, Morenza JL. Liquids microprinting through laser-induced forward transfer. *Appl Surf Sci*; 2009;255.
- [11] Duocastella M, Fernandez-Pradas J, Morenza JL, Serra P. Time-resolved imaging of the laser forward transfer of liquids. *J Appl Phys* 2009;106: 084907.
- [12] Lin Y, Huang Y, Chrisey DB. Droplet formation in matrix-assisted pulsed-laser evaporation direct writing of glycerol-water solution. *J Appl Phys* 2009;105:093111–6.
- [13] Guillemot F, Souquet A, Catros S, Guillotin B, Lopez J, Faucon M, et al. High-throughput laser printing of cells and biomaterials for tissue engineering. *Acta Biomater* 2010;6:2494–500.
- [14] Dincă V, Ranella A, Popescu A, Dinescu M, Farsari M, Fotakis C. Parameters optimization for biological molecules patterning using 248-nm ultrafast lasers. *Appl Surf Sci* 2007;254:1164–8.
- [15] Nakamura M, Kobayashi A, Takagi F, Watanabe A, Hiruma Y, Ohuchi K, et al. Biocompatible inkjet printing technique for designed seeding of individual living cells. *Tissue Eng Part A* 2005;11:1658–66.
- [16] Barron JA, Krizman DB, Ringeisen BR. Laser printing of single cells: statistical analysis, cell viability, and stress. *Ann Biomed Eng* 2005;33:121–30.
- [17] Norotte C, Marga FS, Niklason LE, Forgacs G. Scaffold-free vascular tissue engineering using bioprinting. *Biomaterials* 2009;30:5910–7.
- [18] Engler AJ, Sen S, Sweeney HL, Discher DE. Matrix elasticity directs stem cell lineage specification. *Cell* 2006;126:677–89.
- [19] Klebe RJ. Cytoscribing: a method for micropositioning cells and the construction of two- and three-dimensional synthetic tissues. *Exp Cell Res* 1988;179:362–73.
- [20] Klebe RJ, Thomas CA, Grant GM, Grant A, Gosh P. Cytoscription: computer controlled micropositioning of cell adhesion proteins and cells. *Methods Cell Sci* 1994;16:189–92.
- [21] Ahmed TA, Dare EV, Hincke M. Fibrin: a versatile scaffold for tissue engineering applications. *Tissue Eng Part B Rev* 2008;14:199–215.
- [22] Cui X, Boland T. Human microvasculature fabrication using thermal inkjet printing technology. *Biomaterials* 2009;30:6221–7.
- [23] Xu T, Jin J, Gregory C, Hickman JJ, Boland T. Inkjet printing of viable mammalian cells. *Biomaterials* 2005;26:93–9.
- [24] Wu PK, Ringeisen BR. Development of human umbilical vein endothelial cell (HUVEC) and human umbilical vein smooth muscle cell (HUVSMC) branch/stem structures on hydrogel layers via biological laser printing (BioLP). *Biofabrication* 2010;2:014111.
- [25] Yamada KM, Cukierman E. Modeling tissue morphogenesis and cancer in 3D. *Cell* 2007;130:601–10.
- [26] Fernandes TG, Diogo MM, Clark DS, Dordick JS, Cabral JMS. High-throughput cellular microarray platforms: applications in drug discovery, toxicology and stem cell research. *Trends Biotechnol* 2009;27:342–9.
- [27] Bruzewicz DA, McGuigan AP, Whitesides GM. Fabrication of a modular tissue construct in a microfluidic chip. *Lab Chip* 2008;8:663–71.
- [28] Albrecht DR, Underhill GH, Wassermann TB, Sah RL, Bhatia SN. Probing the role of multicellular organization in three-dimensional microenvironments. *Nat Methods* 2006;3:369–75.
- [29] Anderson DG, Putnam D, Lavik EB, Mahmood TA, Langer R. Biomaterial microarrays: rapid, microscale screening of polymer–cell interaction. *Biomaterials* 2005;26:4892–7.
- [30] Taff BM, Voldman J. A scalable addressable positive-dielectrophoretic cell-sorting array. *Anal Chem* 2005;77:7976–83.
- [31] Lee M, Kumar RA, Sukumaran SM, Hogg MG, Clark DS, Dordick JS. Three-dimensional cellular microarray for high-throughput toxicology assays. *Proc Natl Acad Sci U S A* 2008;105:59–63.
- [32] Chen C, Barron J, Ringeisen B. Cell patterning without chemical surface modification: cell-cell interactions between printed bovine aortic endothelial cells (BAEC) on a homogeneous cell-adherent hydrogel. *Appl Surf Sci* 2006;252:8641–5.
- [33] Voldman J. Engineered systems for the physical manipulation of single cells. *Curr Opin Biotechnol* 2006;17:532–7.
- [34] Duncan AC, Weisbuch F, Rouais F, Lazare S, Baquey C. Laser microfabricated model surfaces for controlled cell growth. *Biosens Bioelectron* 2002;17:413–26.
- [35] Liu Tsang V, Chen AA, Cho LM, Jadin KD, Sah RL, DeLong S, et al. Fabrication of 3D hepatic tissues by additive photopatterning of cellular hydrogels. *FASEB J* 2007;21:790–801.
- [36] Claeysseens F, Hasan EA, Gaidukeviciute A, Achilleos DS, Ranella A, Reinhardt C, et al. Three-dimensional biodegradable structures fabricated by two-photon polymerization. *Langmuir* 2009;25:3219–23.
- [37] Lazare S, Tokarev V, Sionkowska A, Wiśniewski M. Surface foaming of collagen, chitosan and other biopolymer films by KrF excimer laser ablation in the photomechanical regime. *Appl Phys A: Mater Sci Process* 2005;81:465–70.
- [38] Hopp B, Smasz T, Kresz N, Barna N, Bor Z, Kolozsvári L, et al. Survival and proliferative ability of various living cell types after laser-induced forward transfer. *Tissue Eng Part A* 2005;11:1817–23.
- [39] Barron JA, Ringeisen BR, Kim H, Spargo BJ, Chrisey DB. Application of laser printing to mammalian cells. 1. *Thin Solid Films* 2004;453–454:383–7.
- [40] Othon CM, Wu X, Anders JJ, Ringeisen BR. Single-cell printing to form three-dimensional lines of olfactory ensheathing cells. *Biomed Mater* 2008;3:034101.
- [41] Ringeisen BR, Kim H, Barron JA, Krizman DB, Chrisey DB, Jackman S, et al. Laser printing of pluripotent embryonal carcinoma cells. *Tissue Eng Part A* 2004;10:483–91.
- [42] Koch L, Kuhn S, Sorg H, Gruene M, Schlie S, Gaebel R, et al. Laser printing of skin cells and human stem cells. *Tissue Eng Part C Methods* 2009;12: 091221133515000.